Tetrazane: Hartree−Fock, Gaussian-2 and -3, and Complete Basis Set Predictions of Some Thermochemical Properties of N$_4$H$_6$

David W. Ball

Department of Chemistry, Cleveland State University, Cleveland, Ohio 44115

Received: July 26, 2000; In Final Form: October 16, 2000

Optimized geometries, vibrational frequencies, conformation energies, heats of formation, and proton affinities for tetrazane, H$_2$N−NH−NH−NH$_2$, are determined using various-level ab initio methods. Consequences for tetrazane's role as a high-energy material are discussed.

Introduction

According to Greenwood and Earnshaw,[1] nitrogen and hydrogen make at least seven binary compounds, the most well-known being ammonia, NH$_3$. Hydrazine, N$_2$H$_4$, is used as a fuel, and the salt hydrazinium azide (N$_2$H$_5$$^+N_3$$^-$) also qualifies as a binary N/H compound. Two other azide compounds, hydrogen azide (HN$_3$) and ammonium azide (NH$_4$N$_3$), are included on the list, which is rounded out by diimide (also called diazene), N$_2$H$_2$, and tetrazene, H$_2$N−N=N−NH$_2$. Diimide and tetrazene were most recently isolated. N$_2$H$_2$ had been proposed as a reaction intermediate in the reduction of olefinic and acetylenic bonds by Corey et al.[2] Its infrared spectrum was first probed by Van Thiel and Pimentel et seq.[3] in cryogenic matrices, and purportedly in solid form by Trombetti[4] in 1971. Its first unequivocal isolation was in 1972, when Wiberg, Bachhuber, and Fischer[5] thermally decomposed tosylhydrazide salts at low pressures (<10^{-4} Torr) and condensed N$_2$H$_2$ at liquid oxygen temperatures (−183 °C). Later, Willis and Back[6] showed that N$_2$H$_2$ was relatively stable kinetically, decomposing in the gas phase with a half-life of several minutes. They suggested that diimide might therefore be an important intermediate in hydronitrogen chemistry. Since its isolation, several hundred studies on diimide have been published.

Tetrazene was first isolated in 1975 by Wiberg, Bayer, and Bachhuber.[7] Prepared at −78 °C, it is stabler than diimide but still decomposes at temperatures higher than 0 °C, either by reacting to N$_2$ and N$_2$H$_4$ or isomerizing to ammonium azide. The crystal structure of tetrazene at −90 °C[8] showed that the *trans* isomer is formed exclusively. In fact, for both diimide and tetrazene, the *trans* isomer has been characterized, but the *cis* isomer has not been conclusively isolated.

The fully saturated version of tetrazene is tetrazane, H$_2$N−NH−NH−NH$_2$. Tetrazane has been postulated to be an intermediate in the decomposition of hydrazine[9] and was thought to be isolated by Rice and Sherber.[10] They based their supposition on the decomposition of a hydrazine pyrolysis product, which decomposed into a 2:3 ratio of nitrogen and hydrogen. However, no other direct evidence was presented. More recently, tetrazane has been postulated as an intermediate in the pulse-radiolysis-induced decomposition of hydrazine by hydroxyl radicals.[11]

If tetrazane's isolability ever is established, doubtless it will belong to the class of high-energy compounds. This was illustrated by Dasent,[12] whose bond-energy analysis provided an estimate of +89 kcal/mol for ΔH_f [tetrazane]. New high-energy compounds are of constant interest as potential explosives and/or fuels; witness the recent interest in polynitrocubane chemistry.[13] Therefore, we have conducted a study on the thermochemical properties of tetrazane, N$_4$H$_6$. In particular, we applied high-level Gaussian-2, Gaussian-3, and complete basis set (CBS) techniques to determine optimized geometries, conformational energy diagrams, heats of formation, and proton affinities.

Calculational Details

Optimized parameters and single-point energy values were determined with the GAUSSIAN 98 program.[14] The calculations were performed on an SGI Origin 2000 or Cray SV1 supercomputer located at the Ohio Supercomputer Center in Columbus, Ohio. Depending on the goal of the calculation (i.e., optimization of geometry, relative energy of conformations, heat of formation, etc.), different methods and basis sets were used, which will be discussed in the appropriate section of the Results. G2,[15] G3,[16] and various CBS[17] methods were utilized as provided by the software.

Results and Discussion

The hydrocarbon equivalent of tetrazane is butane. The structure of butane and the energetic consequences of its conformations is a major topic in first-year organic chemistry. In tetrazane, however, the lone electron pair on each nitrogen introduces the possibility of stereoisomerism at N2 and N3 of the chain. With two stereocenters, tetrazane can have a maximum of 2^2 = 4 stereoisomers. However, only three stereoisomers exist as unique structures. Using the "*R/S*" labels adopted from organic chemistry, the three structures can be labeled (*R,S*), (*R,R*), and (*S,S*). The (*R,R*) and (*S,S*) stereoisomers are enantiomers of each other (i.e., nonsuperimposable mirror images), and so will have identical thermochemical behavior. The (*R,S*) stereoisomer is a diastereomer (i.e., a nonsuperimposable stereoisomer) to the other two isomers, and will have a different thermochemical behavior. Since the (*R,S*) stereoisomer is its own mirror image (a "meso" compound, to borrow nomenclature from organic chemistry), it does not have an enantiomer. Therefore, there are only two independent stereoisomers of tetrazane. Whether or not two (or more) distinct isomers would actually exist depends on the inversion barrier at the stereocenters. We will consider the different isomers in determination of minimum-energy structures and conformations, but not in the determination of other thermochemical quantities (differences which we expect will be minor).
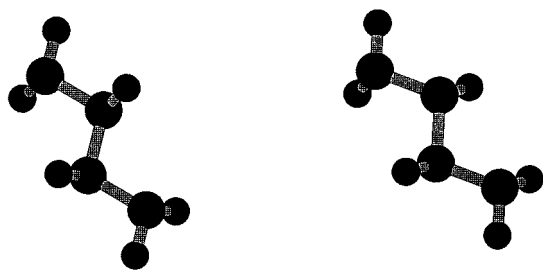
Figure 1. Initial geometries of *cis-* (left) and *trans*-tetrazane (right) for geometry optimizations. These initial geometries are intended to mimic minimum-energy hydrocarbon conformation. The relative positions of thee hydrogens on N2 and N3 are used to differentiate the *cis* isomer from the *trans* isomer.
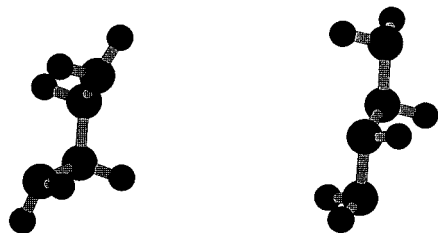

Figure 2. Optimized geometries of the *cis-* (left) and *trans*-tetrazane (right). Curiously, the optimized geometry of the stereoisomer originally defined as *cis* has the defining hydrogens on opposite sides of the central N−N bond, whereas the stereoisomer originally defined as *trans* has the defining hydrogens on the same side of the central N−N bond.

TABLE 1: HF/6-31G* Optimized Geometric Parameters of *cis-* and *trans*-tetrazane (C_2 Point Group)

parameter[a]	*cis*-tetrazane	*trans*-tetrazane
r(N1−N2)	1.411	1.437
r(N2−N3)	1.391	1.409
r(N1−H1)	0.998	1.004
r(N1−H2)	1.002	1.003
r(N2−H3)	1.001	1.006
α(H1−N1−H2)	109.2	105.3
α(N1−N2−N3)	111.9	105.6
α(N1−N2−H3)	111.1	105.3
δ(N1−N2−N3−N4)	51.4	178.1
δ(H1−N1−N2−H3)	90.6	74.0

[a] H1, H2 bonded to N1; H3 bonded to N2; etc. All distances in Å, all angles in degrees.

Geometries and Conformational Energies. Starting from a classic "all-staggered" conformation, the (R,S) conformation of tetrazane has the lone hydrogens on N2 and N3 on opposite sides of the nitrogen backbone. We will refer to this as the trans isomer of tetrazane. The (R,R) [and (S,S)] conformation has the N2 and N3 hydrogens on the same side of the N backbone; we will refer to this as the cis isomer. Figure 1 shows the initial geometries of *trans-* and *cis*-tetrazane that were used in the optimizations.

Figure 2 shows the optimized geometries of *cis-* and *trans*-tetrazane, as calculated using HF/6-31G* methods. In both cases, the chain backbone twisted in such a way as to apparently minimize the overlap of the lone electron pairs on each nitrogen. The end result is that *cis*-tetrazane adopts a geometry in which the hydrogens on N2 and N3 are trans to each other, whereas *trans*-tetrazane adopts a geometry in which the N2 and N3 hydrogens are cis to each other. Both geometries were constrained to C_2 point group symmetry (symmetry elements E and C_2). Table 1 lists the optimized geometric parameters of *cis-* and *trans*-tetrazane. None of the bond distances or parameters are out of the ordinary, although the bond angles in *cis*-tetrazane are slightly larger than normal for nitrogen centers.

TABLE 2: Predicted Frequencies (cm^{-1}), Intensities (km/mol), and Approximate Descriptions of *cis-* and *trans*-Tetrazane

cis-tetrazane		*trans*-tetrazane	
247 (3)	NNNN bend	104 (14)	NNNN bend
315 (99)	NH$_2$ wag	188 (139)	NH$_2$ wag
362 (53)	NNNN def	203 (16)	NNNN def
492 (1)	NHNH wag	360 (7)	NNNN bend
688 (22)	NNN bend	559 (2)	NNN bend
945 (32)	NN str	1032 (20)	NN str
996 (66)	NNN bend	1160 (35)	asym NN str
1039 (99)	NN str	1172 (29)	NH wag
1097 (181)	NH wag	1187 (242)	NH bend
1190 (30)	asym NNNN str	1249 (2)	NN str
1240 (42)	NHNH wag	1300 (25)	NN str/NH$_2$ wag
1379 (27)	NN str	1332 (12)	NHNH def
1444 (5)	NH$_2$ twist	1491 (8)	NH$_2$ twist
1450 (10)	NNH bend	1504 (1)	NHNH twist
1621 (2)	sym HNNH bend	1666 (1)	asym HNNH bend
1743 (2)	asym HNNH bend	1697 (9)	sym HNNH bend
1831 (30)	sym NH$_2$ bend	1825 (29)	asym NH$_2$ bend
1848 (13)	asym NH$_2$ bend	1827 (53)	sym NH$_2$ bend
3716 (2)	sym NH$_2$ str	3663 (14)	asym NH str
3720 (5)	sym NH$_2$ str	3684 (1)	sym NH str
3750 (4)	sym NH str	3701 (2)	sym NH$_2$ str
3773 (1)	asym NH str	3702 (2)	sym NH$_2$ str
3832 (4)	asym NH$_2$ str	3791 (2)	asym NH$_2$ str
3832 (1)	asym NH$_2$ str	3790 (2)	asym NH$_2$ str

Table 2 lists the (unscaled) vibrational frequencies of each isomer, along with a rough description of each mode. Some of the descriptions are rather rough, given the complexity of the particular normal mode. There are no major differences in the predicted vibrational spectra, although many of the modes in the trans isomer are slightly lower in energy than the equivalent mode in the cis isomer. There are near degeneracies in several of the modes, especially in the NH and NH$_2$ stretches. Both stretching motions also exhibit symmetric and asymmetric counterparts; i.e., in the symmetric NH stretch, the two N−H bonds (at N2 and N3) are stretching in-phase, while for the asymmetric NH stretch, the two N−H bonds are stretching out-of-phase. There are two nearly-degenerate normal modes for the symmetric NH$_2$ stretch and the asymmetric NH$_2$ stretch. In each localized normal mode, only one terminal NH$_2$ vibrates substantially.

At this level of calculation (6-31G*), the similarity of the two predicted vibrational spectra might preclude the independent identification of the two separate isomers. However, the values in Table 2 might help differentiate two different isomers in a mixture, or the interconversion of isomers if tetrazane were isolated at low temperatures, as was claimed in the past.[10]

Because tetrazane has all single bonds, there is the potential for free rotation about each N−N bond. The presence of lone electron pairs on each nitrogen should make for an interesting potential energy surface (PES). Rather than consider the complete potential energy surface, we will focus on the potential energy surface generated by rotation of the N2−N3 bond, as this should be different for the cis vs. trans isomer. (We expect that the potential energy surface for terminal NH$_2$ rotation will be very similar to that for hydrazine.) Figures 3 and 4 show the potential energy diagrams (calculated at the HF/6-31G* level) for rotation about the N2−N3 bond for *trans-* and *cis*-tetrazane, respectively. In both cases, the zero point on the energy scale is for the minimum-energy geometry, taken from Table 1. Both figures show a rigid scan, in which all geometric parameters were kept constant during rotation. Figure 4 also shows a PES for a relaxed scan of the cis isomer, in which all other geometric parameters were optimized during the scan. All attempts at
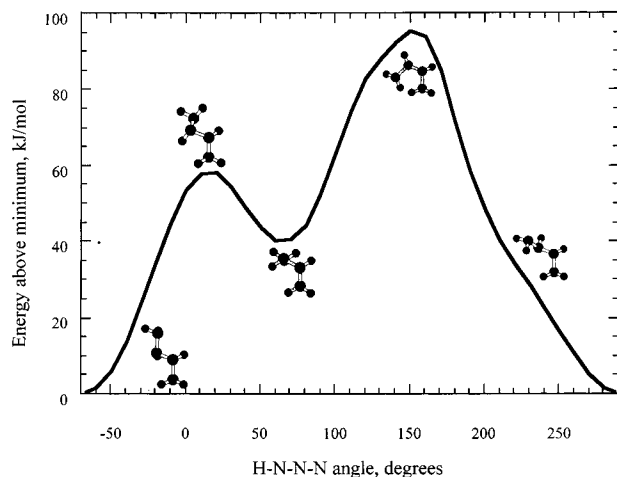
Figure 3. Potential energy surface of *trans*-tetrazane rotation about the central N−N bond. This plot is for a rigid scan. See text for discussion.
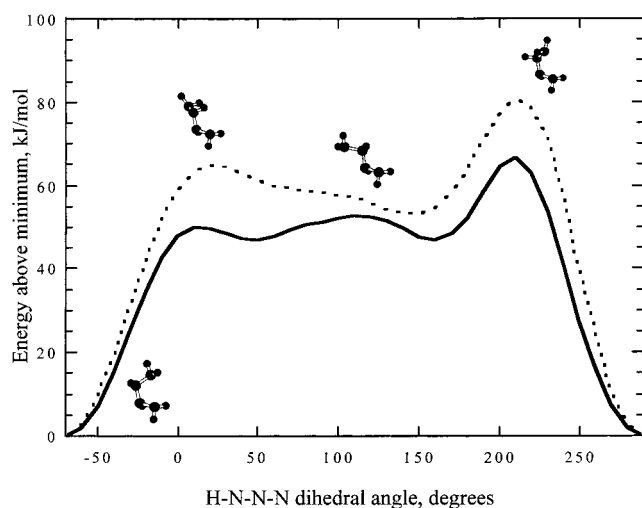

Figure 4. Potential energy surfaces of *cis*-tetrazane rotation about the central N−N bond. The dotted line is a rigid scan, and the solid line shows the surface for a relaxed scan. See text for discussion.

performing a relaxed scan for the trans isomer were unsuccessful because a chiral center would invert during the relaxed scan, generating the more stable cis isomer. However, we should be able to comment on the error in the PES for the trans isomer using Figure 4 as a guide. Graphics of the extrema molecular geometries are superimposed on the energy plots.

There are some qualitative similarities. Maximum barriers to rotation for the cis and trans isomers are calculated as 80 and 95 kJ/mol, respectively, in the rigid scans. The barrier for the cis isomer reduces to ∼65 kJ/mol for the relaxed scan. We suspect that the energy decrease upon relaxation of the trans geometry would be larger in magnitude, but the absolute energy barrier should not be less than that of the cis isomer because the trans isomer is more sterically hindered. We therefore estimate that the energy barrier to rotation would be ∼65−80 kJ/mol for *trans*-tetrazane.

These values compare with an experimental value of ∼19 kJ/mol for butane.[18] While part of the difference is due to calculational vs. experimental values, there should also be a substantial effect due to the opposition of lone electron pairs on N2 and N3. For *trans*-tetrazane, Figure 3 shows that the highest conformational energy is found when the lone electron pairs on N2 and N3 eclipse each other. However, the potential energy plot for *cis*-tetrazane (Figure 4) shows a relative *but not*
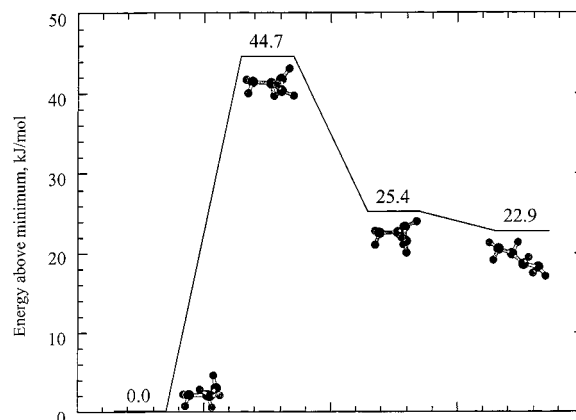

Figure 5. Inversion of the chiral center N2. The hydrogen atom that is inverting is the uppermost hydrogen atom in the minimum-energy molecule, which is *cis*-tetrazane. All of the molecules are pictured so that the left half of the molecule has the same orientation. While the third energy level, at 25.4 kJ/mol above the minimum, is *trans*-tetrazane, it is not in its minimum-energy conformation. The fourth energy level shows that the molecule can reorient to a slightly more stable *trans*-tetrazane.

absolute maximum when the N2 and N3 lone electron pairs eclipse each other. Rather, the absolute maximum on the potential energy curve occurs when the lone electron pairs on N1 and N4 approach each other. While the shape of this curve is doubtless an artifact of the nonrelaxed character of the scan, it does reinforce how the lone electron pairs affect the conformational energy of tetrazane in a way not found in saturated hydrocarbons.

The cis and trans stereoisomers of tetrazane can interconvert by inversion at either N2 or N3, in a way analogous to the inversion of ammonia. The final question to explore is whether these two distinct stereoisomers of tetrazane exist, or if the barrier to inversion is small enough to make the question moot. (At least two stereoisomers of tetrazane, the (*R,R*) and the (*S,S*), must exist.) Starting with optimized cis isomer, the N2 hydrogen was reflected through the N1−N2−N3 plane to simulate inversion, a partial reoptimization was performed by varying structural parameters on only half of the molecule, and this final optimized geometry was used with the cis geometry in a QST2 job (using HF/6-31G*) to find the maximum-energy intermediate between the two geometries. A reaction coordinate plot, annotated with the relevant geometries, is shown in Figure 5. The inverting hydrogen is located at the top right of the structures. An intermediate having planar local geometry about N2 has an energy of 44.7 kJ/mol above the lowest-energy cis conformation. As the hydrogen inverts completely, a metastable trans conformation is found at 25.4 kJ/mol above the cis conformation. A twisting of the other half of the molecule brings the structure to the minimum energy trans geometry, which lies at 22.9 kJ/mol above the cis geometry. Thus we predict a 45 kJ/mol barrier for cis → trans conversion, and a 22 kJ/mol barrier for the trans → cis conversion.

Using simple activated-complex theory, we can use the expression

$$k_{uni} = \frac{k_B T}{h} \frac{q^t}{q} e^{-\Delta U^t / k_B T}$$

to estimate the (high-pressure) unimolecular rate constant for the inversion process. Here, q and q^t are the partition functions of the stable and transition state, respectively, and ΔU^t; is the activation energy barrier. Partition functions are automatically

calculated in as part of a frequency calculation in G9X, so the determination of the unimolecular rate constants is straightforward. For the reaction

$$cis\text{-tetrazan} \underset{k_r}{\overset{k_f}{\rightleftharpoons}} trans\text{-tetrazan}$$
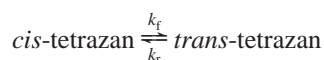
we estimate $k_f = 3.5 \times 10^6$ s^{-1} and $k_r = 1.3 \times 10^{11}$ s^{-1} at 298.15 K. The equilibrium constant K $= k_f/k_r$ equals 2.7×10^{-5} at this temperature.

How do these inversion barriers compare with inversion barriers for other trivalent nitrogen compounds? In a recent review of trivalent nitrogen stereochemistry, Bach and Raban[19] list experimental and calculated inversion barriers for a range of compounds. They note in particular the failure of low-level calculational method to accurately predict inversion barriers, and recommend at least a 6-31G* basis set to get reliable energies in HF calculations. (This is the method presented here.) Ammonia's experimental inversion barrier is 24.2 kJ/mol, whereas that for trimethylamine, N(CH$_3$)$_3$, is 31.4 kJ/mol. Inversion barriers for compounds in which the nitrogen atom is part of a ring are larger: the barrier for aziridine (C$_2$H$_4$NH, the nitrogen analogue of ethylene oxide) is 79.8 kJ/mol. The inversion barrier decreases as the ring size increases, approaching ammoniacal levels in six- and seven-membered cycloaliphatic compounds. The only multi-N compounds that Bach and Raban consider are triaziridines, (*cyclo*-NR)$_3$. They report an HF/6-31G*-calculated barrier of 51.8 kJ/mol for (NH)$_3$. Jennings and Boyd[20] report on diaziridines (*cyclo*-CH$_2$(NR)$_2$) and triaziridines in more detail and note that the substitution of nitrogens for carbons in rings increases the inversion energy for each nitrogen, due to lone pair repulsion effects. However, larger groups attached to the nitrogens actually lower the inversion barrier, usually due to interaction between the groups and the lone electron pair on the nitrogen. Thus, the inversion barriers presented here are commensurate with barriers for other compounds, including compounds that have adjacent nitrogens.

Heats of Formation. Using the HF/6-31G*-optimized geometry of *cis*-tetrazane (the lower energy of the two stereoisomers) from Figure 2 as the initial geometry, high-level ab initio calculations were performed to determine the heat of formation of tetrazane. G2, G3, and CBS methods were employed here because of their well-documented ability to predict energies (within ca. <2 kcal/mol).

Three different gas-phase chemical reactions were used to determine the heat of formation of tetrazane. The first is an isodesmic reaction defined to have the same number of bonds (N−H, N−N) on both sides of the reaction:

$$3N_2H_4 \rightarrow N_4H_6 + 2NH_3 \qquad (1)$$

The second is the reverse of the atomization reaction for tetrazane:

$$4N\ (^4S) + 6H\ (^2S) \rightarrow N_4H_6\ (^1S) \qquad (2)$$

For these first two reactions, the enthalpy change for the reaction as written was first determined from the calculated energies of the species. Then, this enthalpy change was combined with the measured heats of formation for N$_2$H$_4$ and NH$_3$ (for reaction 1[21]) or for N and H (for reaction 2[22]) in the proper stoichiometric ratios to determine ΔH_f [N$_4$H$_6$]. The third reaction the heat of formation reaction as defined by the formation of a compound from its elements under standard conditions:

$$2N_2 + 3H_2 \rightarrow N_4H_6 \qquad (3)$$
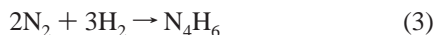
In this case, ΔH_f [N$_4$H$_6$] was determined by a direct stoichiometric combination of the calculated energies of the products and reactants.

To compare methods, Table 3 illustrates how accurate reactions 2 and 3 are in determining the heats of formation for NH$_3$ and N$_2$H$_4$. (The isodesmic reaction method for calculating ΔH_f is omitted.) For ammonia, the table shows good agreement for most methods, with an average variance of 3.9 kJ/mol, or less than 1 kcal/mol. The largest variances were 8.3 and 7.4 kJ/mol for the CBS−QB3 method using the atomization reaction, and 8.3 kJ/mol for the CBS-*q* method using the formal formation reaction. The three highest-cost methods (CBS-APNO, G2, and G3) all predicted slightly higher ΔH_f than experiment, whereas the rest of the methods generally split being above or below the experimental value of ΔH_f for ammonia. For hydrazine, the average variance is 7.4 kJ/mol, still under the 2 kcal/mol limit, but almost twice as high as the variance for ammonia. In this case, the variance was almost always positive, suggesting that these calculations and reactions might overestimate the heat of formation of hydronitrogen compounds.

Table 4 lists the heats of formation of tetrazane by reaction and by method. Three of the values (the CBS-*q* method using reaction 1 and the original and modified CBS-4 methods applied to reaction 3) are rather lower than most of the predicted values, which lie between 281 and 304 kJ/mol. Neglecting these three low values, the isodesmic reaction 1 generally predicts a slightly lower ΔH_f than the atomization reaction 2 or the heat of formation reaction 3. With the exception of the three low values, there is good agreement for the predicted ΔH_f [N$_4$H$_6$] among the calculational methods within each type of reaction used, with reactions 1−3 exhibiting a 7, 11, and 6 kJ/mol range in ΔH_f, respectively. This consistency in result suggests that use of each reaction embodies some different systematic error (i.e., experimental value of ΔH_f or enthalpy of atomization, etc.) is involved. It is disturbing that the different reaction schemes are not more consistent with each other. Schlegel and Skancke[24] reported ΔH_f for NH$_2$, NH$_3$, N$_2$H$_4$, N$_3$H$_5$, and N$_4$H$_6$ (triaminoammonia) using the G2 method based on a heat of formation reaction and an atomization reaction, and found variations ranging from 1.7 to 3.7 kJ/mol between the two reactions. They did not report heats of formation using an isodesmic reaction. The respective G2 values for ΔH_f [tetrazane] reported here mimic this level of agreement, although curiously the G3 values do not.

According to benchmarks,[17,23] the CBS−APNO and −Q methods are the most accurate complete basis set method (with CBS−APNO being the most computationally expensive as well). Since G2 and G3 theory are also promoted as high-accuracy methods,[15,16] perhaps the best comparison would focus on those four methods. The use of isodesmic and heat of formation reactions provided the more consistent values of ΔH_f [N$_4$H$_6$], with ranges of 2.6 and 5.0 kJ/mol, respectively. The range among the four methods using the atomization reaction is 12.0 kJ/mol. Thus, a value of 293 ± 10 kJ/mol (70.0 ± 2.5 kcal/mol) would seem a reasonable value for the ΔH_f of tetrazane. This is significantly lower than Dasent's estimate,[12] based on approximations of bond energies, of 88.9 kcal/mol. This also compares to values of 74.3 kcal/mol (formation reaction-based) and 73.9 kcal/mol (atomization reaction-based) for ΔH_f of triaminoammonia, the branched isomer of N$_4$H$_6$, as determined by Schlegel and Skancke.[24]

Table 5 lists the heats of formation for the first four "straight-chain" compounds of the series N$_n$H$_{n+2}$. For N$_3$H$_5$ and N$_4$H$_6$, only calculated values are available. Each homologue differs

TABLE 3: Calculated ΔH_f (kJ/mol) for Ammonia and Hydrazine

reaction	CBS-q	CBS-Q	CBS-4o	CBS-4m	CBS$-$QB3	CBS$-$APNO	G2	G3
NH$_3$								
[2]	-48.4	-38.9	-48.9	-49.2	-38.5	-44.8	-41.0	-44.0
[3]	-54.2	-41.3	-40.5	-42.7	-43.4	-44.7	-44.7	-42.1
N$_2$H$_4$								
[2]	105.4	105.1	84.0	84.7	105.7	99.3	102.9	99.3
[3]	101.1	104.8	102.1	99.6	100.4	101.2	99.7	104.8

TABLE 4: Calculated ΔH_f (kJ/mol) for Tetrazane

reaction	CBS-q	CBS-Q	CBS-4o	CBS-4m	CBS$-$QB3	CBS$-$APNO	G2	G3
[1]	262.8	281.0	283.9	287.4	282.6	283.7	281.4	283.4
[2]	296.4	300.0	293.3	293.7	292.6	298.7	292.0	303.9
[3]	297.8	296.2	255.7	261.7	298.5	293.1	294.0	291.1

TABLE 5: Trend in ΔH_f for N$_n$H$_{n+2}$

compound	ΔH_f, kJ/mol	source
NH$_3$	-45.9	expt.[21]
N$_2$H$_4$	95.4	expt.[21]
N$_3$H$_5$	ca. 200	calc.[25]
N$_4$H$_6$	293	calc., this work

from its neighbors by an NH unit. Accordingly, there should be some trend in the thermodynamics of formation. Table 5 shows that, for what information is available, a trend has not yet been established. The change in ΔH_f going from NH$_3$ to N$_2$H$_4$ is 141.3 kJ, from N$_2$H$_4$ to N$_3$H$_5$ is about 105 kJ/mol, and from N$_3$H$_5$ to N$_4$H$_6$ is about 93 kJ/mol. In comparison, for normal aliphatic hydrocarbons, ΔH_f data[21] show that the *difference* in the heats of formation for CH$_4$ and C$_2$H$_6$ is -9.2 kJ/mol, but thereafter the change in ΔH_f is fairly constant for adjacent homologues at -20.5 to -20.9 kJ/mol. That is, the addition of a CH$_2$ to any homologue changes its ΔH_f by about -20.5 kJ/mol, and this trend is firmly established by the addition of a *second* CH$_2$ to the parent homologue (i.e., CH$_4$). The data for N$_n$H$_{n+2}$ suggest that the differences in ΔH_f are approaching some constant change for each NH added, but that a constant difference has not been established yet upon reaching the fourth member of the series. Given the limited number of data points, it may be premature to predict what the difference in ΔH_f will be, but if the difference continues to drop to 1/3 of its previous value as we continue through the series, then the change in ΔH_f would approach 85$-$87 kJ/mol for subsequent NH additions, and should be reached by the seventh or eighth member of the series (N$_7$H$_9$ or N$_8$H$_{10}$).

A comparison of the calculated ΔH_f's of tetrazane and its branched isomer, triaminoammonia, show that the straight-chain isomer is more stable by ca. 17 kJ/mol. This is in contrast with the trends seen in hydrocarbons. Typically, branched isomers (more specifically, methyl-*n*-alkanes) are *more* stable than their isomeric *n*-alkanes, by 6$-$9 kJ/mol. The presence of a lone electron pair on each nitrogen is no doubt the culprit. Triaminoammonia is more structurally compact, bringing four lone electron pairs into rather close proximity. In tetrazane, the lone electron pairs can be distributed farther apart in space; indeed, Figure 2 shows that the stable conformations of tetrazane orient themselves to minimize lone-electron-pair repulsion. The addition of more lone electron pairs, making longer and longer N$_n$H$_{n+2}$ chains, contributes to a progressively less stable molecule, as indicated by the increase in ΔH_f.

At 293 kJ/mol, the heat of formation of tetrazane is high but not extremely so. We can compare it to the heats of formation of cyanogen (74 kJ/mol), cubane (622 kJ/mol), and xenon trioxide (402 kJ/mol). Curiously, the heat of formation of tetrazane is rather similar to the heat of formation of hydrogen azide, HN$_3$, another hydronitrogen compound: ΔH_f [HN$_3$,l] = 264 kJ/mol, whereas ΔH_f [HN$_3$,g] = 294 kJ/mol. (The boiling point of hydrogen azide is 37 °C.) The potential applicability of tetrazane as a high-energy material awaits information about its kinetic stability and its condensed-phase density.

Proton Affinities. The proton affinity (PA) of a compound is defined as the negative of the ΔH_{rxn} for the gas-phase acceptance of a proton:

$$B(g) + H^+(g) \rightarrow BH^+(g) \qquad -\Delta H = PA \qquad (4)$$
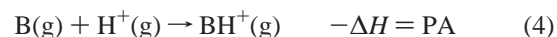
Proton affinity is a measure of how well a compound acts as a base, and the information provides a useful comparison of the chemical properties of related compounds. In fact, ammonia is one of the historical standards used to establish a proton affinity scale. According to Lias, Liebman, and Levin,[26] use of ammonia as a standard is more tradition than good reproducible science due to variation in experimental values for PA (NH$_3$), which has a selected value of 853.5 kJ/mol. Jursic[27] has used the CBS$-$Q method to calculate a PA for ammonia of 848 kJ/mol, a relative error of -0.6% and well within the 2 kcal/mol limit.

Tetrazane has two different sites to bond with an H$^+$, N1 (equivalent to N4), and N2 (equivalent to N3). Because it is expected that each site will have a different proton affinity, geometry optimizations were performed on NH$_2$(NH)$_2$NH$_3^+$ and NH$_2$NHNH$_2^+$NH$_2$. Proton affinities were determined by comparing electronic energies only; no correction for thermal energies was made. Calculated PAs are listed in Table 6, for each method and site of protonation. First, we comment on the magnitude of the calculated PAs. Relatively speaking, they are extremely high, ranging between 1072 and 1112 kJ/mol. To put this in perspective, recall that PA [NH$_3$] is a mere 853.5 kJ/mol. Also, in the list of proton affinities by Lias et al.,[26] the highest proton affinity listed is for N,N,N′,N′-tetramethyl-1,8-naphthalenediamine, whose PA is 1012 kJ/mol. (Indeed, many nitrogenous compounds have PAs larger than NH$_3$, as shown in ref 26.) Even inclusion of thermal energy corrections would not bring the calculated PAs for tetrazane down to this value. Furthermore, Table 7 lists PAs of N$_n$H$_{n+2}$ for comparison. The PA for N$_2$H$_4$ is very similar to that of ammonia, and the

TABLE 6: Calculated Proton Affinities (kJ/mol) for Tetrazane

Protonation site	CBS-q	CBS-Q	CBS-4o	CBS-4m	CBS$-$QB3	CBS$-$APNO	G2	G3
N1	1097	1094	1095	1106	1092	1112	1093	1094
N2	1085	1089	1085	1084	1085	1089	1072	1088

TABLE 7: Trend of PAs for N_nH_{n+2}

compound	PA, kJ/mol	source
NH_3	853.5	expt.[26]
N_2H_4	856	expt.[26]
N_3H_5	ca. 866, 876	calc.[25]
N_4H_6	ca. 1085, 1094	calc., this work

PA for triazane is about 20 kJ/mol higher. (Note that triazane, NH_2NHNH_2, also has two distinct sites for protonation.) Our results show an increase in PA of over 200 kJ/mol when going from N_3H_5 to N_4H_6. Why this tremendous increase?

Examination of the optimized geometry of the protonated molecule is suggestive. Figure 2, the optimized geometries of neutral tetrazane, shows that the molecule orients itself to minimize the repulsion of the N lone electron pairs, but nonetheless the minimum-energy geometries do not adopt a perfect staggered-conformation, all-trans backbone like their hydrocarbon counterparts. Inspection of the protonated molecular geometry shows some distinct differences compared to the neutral parent molecule. The N center(s) adjacent to the protonation site adopt an almost perfect staggered conformation with respect to the protonated N. This almost certainly increases the amount of hyperconjugation between lone electron pairs and the σ^* orbitals on adjacent N–H bonds. Such effects have already been implicated in the stabilization of triazane over hydrazine.[24] The geometries show that the molecule does not contort itself so that there is interaction between the additional proton and another lone pair of the molecule. This geometric rearrangement may be partly responsible for the dramatic increase in PA of tetrazane over other homologues.

Protonation at N1 is slightly energetically preferred over protonation at N2. But as with the ΔH, there is some variability in the value for the PAs of tetrazane depending method. For this chemical process, extreme variations are found for one CBS–APNO and one G2 calculation. This is rather surprising, because both of these methods are touted as being among the more accurate. Most methods predict a PA of 1094 ± 2 kJ/mol for the terminal nitrogen sites, and 1085 ± 2 kJ/mol for the middle nitrogen site.

N–N bond distances increase upon protonation, in some calculations markedly (to ca. 1.5 Å). This suggests a possible pathway for decomposition of the high-energy molecule, via N–N scission.

Conclusion

We have investigated the thermochemical properties of tetrazane, $NH_2NHNHNH_2$, using various CBS and Gaussian-n methods. Structurally, tetrazane exists as three different stereoisomers, but energy, rate constant, and equilibrium constant calculations suggest that at room temperature the molecule should exist predominantly as enantiomeric (R,R) and (S,S) isomers (referred to in this paper as the cis isomer). Potential energy curves for rotation about N–N bonds are more complicated and less regular that the potential energy curve for butane, the hydrocarbon equivalent. Calculated vibrational spectra suggest that the difference in isomers might be detectable at temperatures low enough to inhibit inversion. The heat of formation of tetrazane was calculated as 293 ± 10 kJ/mol. Tetrazane has two different sites for protonation and thus two different proton affinities. The PAs were calculated as 1085 and 1094 kJ/mol. These are very large values and represent a large increment with respect to its homologues in the N_nH_{n+2} series.

References and Notes

(1) Greenwood, N. N.; Earnshaw, A. *The Chemistry of the Elements* Pergamon Press: Oxford, 1984.

(2) Corey, E. J.; Mock, M. L.; Pasto, D. J. *J. Am. Chem. Soc.* **1961**, *83*, 2957.

(3) Van Thiel, M.; Pimentel, G. C. *J. Chem. Phys.* **1960**, 32, 133. Rosengren, K. J.; Pimentel, G. C. *J. Chem. Phys.* **1965**, *43*, 507.

(4) Trombetti, A. *J. Chem. Soc. A* **1971**, 1086.

(5) Wiberg, N.; Bachhuber, H.; Fischer, G. *Angew. Chem., Int. Eng. Ed.* **1972**, *11*, 829.

(6) Willis, C.; Back, R. A. *Can. J. Chem.* **1973**, *51*, 3605.

(7) Wiberg, N.; Bayer, H.; Bachhuber, H. *Angew. Chem.* **1975**, 87, 202.

(8) Veith, M.; Schlemmer, G. *Z. Anorg. Allg. Chem.* **1982**, *494*, 7.

(9) Higginson, W. C. E.; Sulton, D. *J. Chem. Soc.* **1953**, 1042.

(10) Rice, F. O.; Sherber, F. *J. Am. Chem. Soc.* **1955**, *77*, 291.

(11) Hayon, E.; Simic, M. *J. Am. Chem. Soc.* **1972**, *94*, 42.

(12) Dasent, W. E. *Nonexistent Compounds: Compounds of Low Stability* Marcel Dekker: New York, 1965.

(13) Zhang, M.-X.; Eaton, P. E.; Gilardi, R. *Angew. Chem., Int. Ed.* **2000**, *39*, 401.

(14) Frisch, M. J.; Trucks, G. W.; Schlegel, H. B.; Scuseria, G. E.; Robb, M. A.; Cheeseman, J. R.; Zakrzewski, V. G.; Montgomery, J. A., Jr.; Stratmann, R. E.; Burant, J. C.; Dapprich, S.; Millam, J. M.; Daniels, A. D.; Kudin, K. N.; Strain, M. C.; Farkas, O.; Tomasi, J.; Barone, V.; Cossi, M.; Cammi, R.; Mennucci, B.; Pomelli, C.; Adamo, C.; Clifford, S.; Ochterski, J.; Petersson, G. A.; Ayala, P. Y.; Cui, Q.; Morokuma, K.; Malick, D. K.; Rabuck, A. D.; Raghavachari, K.; Foresman, J. B.; Cioslowski, J.; Ortiz, J. V.; Baboul, A. G.; Stefanov, B. B.; Liu, G.; Liashenko, A.; Piskorz, P.; Komaromi, I.; Gomperts, R.; Martin, R. L.; Fox, D. J.; Keith, T.; Al-Laham, M. A.; Peng, C. Y.; Nanayakkara, A.; Gonzalez, C.; Challacombe, M.; Gill, P. M. W.; Johnson, B.; Chen, W.; Wong, M. W.; Andres, J. L.; Gonzalez, C.; Head-Gordon, M.; Replogle, E. S.; Pople, J. A. Gaussian, Inc., Pittsburgh, PA, 1998.

(15) Curtiss, L. A.; Raghavachari, K.; Trucks, G. W.; Pople, J. A. *J. Chem. Phys.* **1991**, *94*, 7221.

(16) Curtiss, L. A.; Raghavachari, K.; Redfern, P. C.; Rassolov, V.; Pople, J. A. *J. Chem. Phys.* **1998**, *109*, 7764.

(17) Ochterski, J. W.; Petersson, G. A.; Montgomery, J. A., Jr. *J. Chem. Phys.* **1996**, *104*, 2598.

(18) McMurry, J. *Organic Chemistry*, 3rd ed. Brooks/Cole Publishing Co: Pacific Grove, CA, 1992.

(19) Bach, R. D.; Raban, M. In *Cyclic Organonitrogen Stereodynamics* Lambert, J. B., Takeuchi, Y., Eds.; VCH: New York, 1992; pp 63–104.

(20) Jennings, W. B.; Boyd, D. R. In *Cyclic Organonitrogen Stereodynamics* Lambert, J. B., Takeuchi, Y., Eds.; VCH: New York, 1992; pp 104–58.

(21) Lide, D. R., ed. *CRC Handbook of Chemistry and Physics*, 71st ed.; CRC: Boca Raton, Florida, **1990**.

(22) Data for $\Delta_f H$ of the gas-phase atom taken from the NIST Chemistry Webbook, http://webbook.nist.gov/chemistry.

(23) Foresman, J. B.; Frisch, Æ. *Exploring Chemistry with Electronic Structure Methods*, 2nd ed.; Gaussian, Inc.: Pittsburgh, PA, 1996.

(24) Schlegel, H. B.; Skancke, A. *J. Am. Chem. Soc.* **1993**, *115*, 7465.

(25) Anthony, D. R.; Ball, D. W., manuscript in preparation.

(26) Lias, S. G.; Liebman, J. F.; Levin, R. D. *J. Phys. Chem. Ref. Data* **1984**, *13*, 695.

(27) Jursic, B. S. *J. Mol. Struct. – THEOCHEM* **1999**, *490*, 1.